

# INTERNATIONAL SOCIETY FOR SOIL MECHANICS AND GEOTECHNICAL ENGINEERING



*This paper was downloaded from the Online Library of the International Society for Soil Mechanics and Geotechnical Engineering (ISSMGE). The library is available here:*

<https://www.issmge.org/publications/online-library>

*This is an open-access database that archives thousands of papers published under the Auspices of the ISSMGE and maintained by the Innovation and Development Committee of ISSMGE.*

# Engineering water repellency in granular solids

Y. Saulick & S.D.N. Lourenço

*Department of Civil Engineering, The University of Hong Kong, Hong Kong*

B.A. Baudet

*Department of Civil, Environmental and Geomatic Engineering, University College London, United Kingdom*

**ABSTRACT:** The use of water repellent granular solids such as soils is an innovative technology for use in applications such as water tight barriers. Synthesising such solids generally necessitate the exclusive use of chemical treatments with little consideration given to the physical characteristics of the solids. This paper summarises the theoretical framework of surface wettability and contact angle by illustrating the classic models developed. The wettability of 3 isolated sieve fractions of a sand was investigated after treatment with dimethyldichlorosilane (DMDCS). The largest contact angle (measured by the sessile drop method) was achieved with the finest fraction (63-212  $\mu\text{m}$ ). Comparison between a flat microscope slide treated with DMDCS and the 63-212  $\mu\text{m}$  fraction showed that the sand had a significantly larger contact angle (a maximum difference of  $20^\circ$ ). This difference was attributed to the particle characteristics which includes particle size, particle shape and surface roughness. The results of the study hint at the possible usage of the physical characteristics of soils in an engineering context to control water repellency.

## 1 INTRODUCTION

Water repellency in granular solids such as soils occur when these solids are not completely wettable. In an agricultural context, a low degree of water repellency is necessary for aggregate stability (Hallett and Young, 1999) while relatively higher extents of water repellency make the soils prone to erosion (King, 1981). In general, silicate minerals present in soils such as quartz are originally wettable (Rodriguez *et al.*, 1997). However, over time in their natural environment, these minerals get coated by organic matter originating from various sources such as decomposed plant material (Ellies *et al.*, 2005).

In geotechnical engineering, the extent to which a soil is wettable is expected to govern its mechanical behaviour under unsaturated conditions. With water repellent soils, liquid bridges from one particle to another are not easily formed; instead the soil particles have discrete micro-droplets nucleating on them. This is demonstrated in Figure 1 where a sand particle treated by dimethyldichlorosilane was subjected to a condensation experiment with an environmental scanning electron microscope. The absence of liquid bridges on particles may inhibit the influence of the capillary stress on the total cohesion (Lourenço *et al.*, 2017) and therefore lead to mechanically weaker soils as observed by Byun *et al.* (2011).

In this paper, the classic models encompassing wettability are illustrated, followed by an investigation of the wetting properties of a flat and a granular solid after chemical treatment.

## 2 CLASSIC MODELS

A drop of liquid deposited on a flat surface will have only three interfacial forces acting on it in an ideal scenario. They are:  $\gamma_{sl}$ ,  $\gamma_{lg}$  and  $\gamma_{sg}$  corresponding respectively to the interfacial force between the solid-liquid, liquid-gas and solid-gas phases. At the three-point interface (Figure 2a), resolving the interfacial forces horizontally along the contact line assuming mechanical equilibrium where the sum of forces equals zero yield the following:

$$-\gamma_{sl} + \gamma_{lg} \cos(180 - CA) + \gamma_{sg} = 0 \quad (1)$$

Rearranging Equation 1 gives:

$$\cos(CA) = \frac{\gamma_{sg} - \gamma_{sl}}{\gamma_{lg}} \quad (2)$$

Equation 2 is known as the Young's equation and the contact angle (CA) is referred to as Young's contact angle ( $CA_Y$ ). The validity of Young's equation re-

quires that the solid surface on which the drop of liquid lies is uniform, smooth, flat, homogenous, inert, insoluble, non-reactive, non-porous and non-deformable (Kwok *et al.*, 1997); conditions which are not met on ‘real’ surfaces. The assumption of non-deformability allows the vertical components of the interfacial forces to be ignored.  $CA_Y$  is not dependent on the nature of the molecular forces as long as the sizes of the drops are large enough (Israelevichvili, 2011).

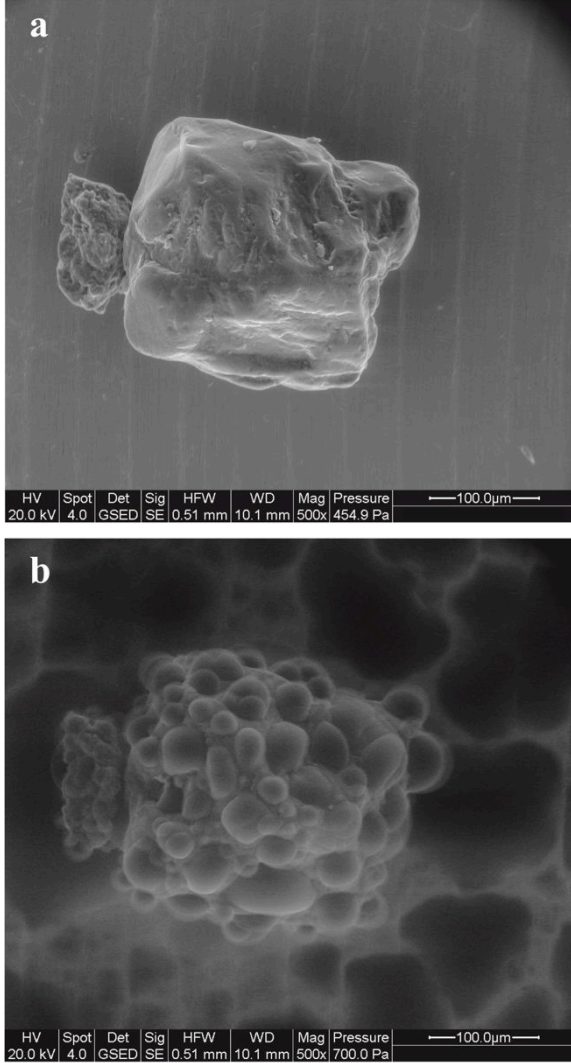


Figure 1. Environmental scanning electron microscope (ESEM) images of a sand particle treated by dimethylchlorosilane: a. before and b. after condensation experiment

The model proposed by Wenzel (1936) modifies the Young's model to take into account the effect of roughness which deviates real surfaces from ideal ones. The same author studied surfaces which differed significantly from flat surfaces to show that wettability depends on how rough a surface is. He proposed to change Equation 2 by a material-independent parameter  $r$  as follows:

$$\cos(CA) = r \frac{\gamma_{sg} - \gamma_{sl}}{\gamma_{lg}} \quad (3)$$

$r$  in Equation 3 is defined as a ratio of the true to the apparent areas and referred to as roughness ratio. The contact angle obtained from the Wenzel model is called the Wenzel contact angle,  $CA_W$ . The model assumes a ‘complete wetting’ where a drop of liquid on the rough surface completely fills the grooves as shown in Figure 2b. The position of the baseline (horizontal dotted line) in Figure 2b is taken to be at the crests of the roughness features. Since  $r \geq 1$ , for a material with  $CA_Y < 90^\circ$ , the resulting  $CA_W$  is less than  $CA_Y$ . On the other hand, if the material initially has a  $CA_Y > 90^\circ$ , the resulting  $CA_W$  is greater than  $CA_Y$ . The effect of varying  $r$  values for different  $CA_Y$  on  $CA_W$  is illustrated in Figure 3. The figure shows the influence of the roughness ratio on the following three values of  $CA_Y$ :  $60^\circ$ ,  $90^\circ$  and  $120^\circ$ . For  $CA_Y = 60^\circ$ , an increase in  $r$  causes a decrease in the resulting  $CA_W$  as demonstrated by the black columns while for  $CA_Y = 120^\circ$ , the opposite trend is observed, i.e. an increase in  $r$  enhances the resulting  $CA_W$  (blue columns). In contrast, for  $CA_Y = 90^\circ$ , varying  $r$  does not influence  $CA_W$ . For the values of  $CA_Y = 60^\circ$  and  $120^\circ$  investigated,  $r = 2.0$  leads to the extreme CA values of  $0^\circ$  and  $180^\circ$  respectively.

The Cassie model considers a wetting regime where a drop of liquid placed on a rough surface does not fill the grooves completely, but instead is in contact with different phases. For the case where the drop of liquid is in contact with two phases, the model is represented as follows:

$$\cos(CA_C) = f_1 \cos(CA_{Y1}) + f_2 \cos(CA_{Y2}) \quad (4)$$

where  $CA_C$  is the Cassie contact angle,  $f_1$  and  $f_2$  are area fractions in contact with phase 1 and phase 2 respectively. The terms  $\cos(CA_{Y1})$  and  $\cos(CA_{Y2})$  represent the cosines of the Young's contact angles of the respective phases. For a very water repellent material, the liquid can arch over from one roughness feature to another and in the process entrapped air beneath it (Figure 2c). Since the contact angle of water with air is equal to  $180^\circ$ , Equation 4 simplifies to the Cassie-Baxter equation (Equation 5) for a porous medium such as soil (Cassie and Baxter, 1944).

$$\cos(CA_C) = f_1 \cos(CA_{Y1}) - f_2 \quad (5)$$

The combination of the Wenzel and Cassie-Baxter models has been carried out in several studies. Recently, Bachmann and McHale (2009) derived a model making use of such a combination. The authors assumed that when a drop liquid bridges from one particle to another, a Cassie-Baxter wetting regime takes place and when the liquid moves onto the particles, it fills in the roughness features completely, i.e. a Wenzel wetting regime occurs. The model

was tested with particles treated with DMDCS and found to be close to the experimental data obtained. The effect of adding DMDCS on a single particle of glass ballotini has been illustrated in Lourenço *et al.* (2017). An overall smoothing of the particle was observed suggesting that the assumption of a Wenzel-like regime on individual particles treated by DMDCS is rational.

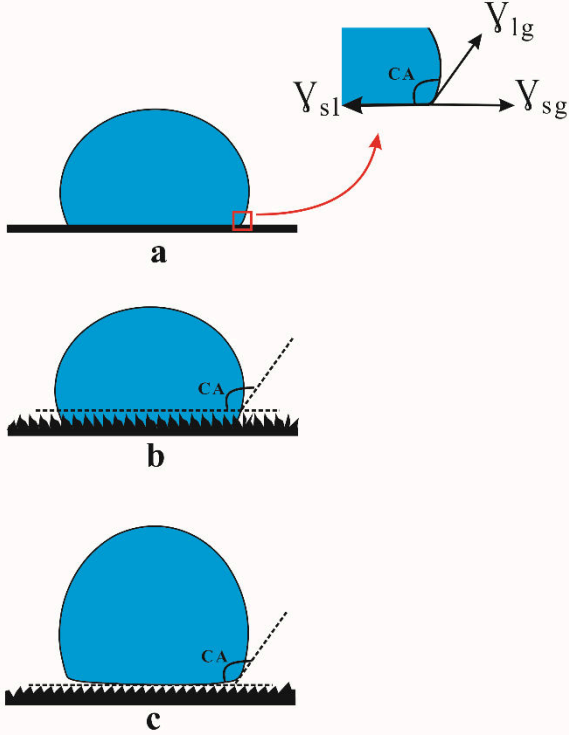


Figure 2. Classic models describing different wetting regimes: a. Young's model ( $CA = CA_Y$ ) b. Wenzel model ( $CA = CA_W$ ) and c. Cassie-Baxter model ( $CA = CA_C$ )

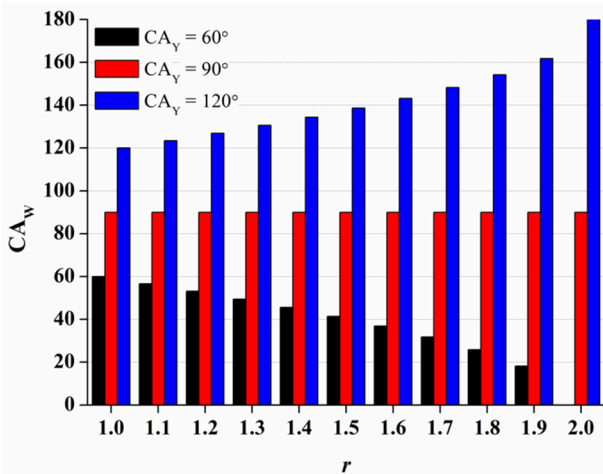


Figure 3. Variation of  $CA_w$  with different  $r$  values for  $CA_Y = 60^\circ, 90^\circ$  and  $120^\circ$ .

### 3 MATERIALS AND METHODS

#### 3.1 Selection and characterisation of solids

Fujian sand, a silica-based sand was sieved and the following sieve fractions ( $\mu\text{m}$ ) were retained for further tests: 63-212, 300-425 and 425-600. The particle characteristics of the sand including its shape

were obtained by a dynamic image analyser (QICPIC; Sympatec GmbH, Clausthal-Zellerfeld, Germany). The device has been implemented in the characterisation of sand particles in several studies (e.g. Yang and Luo, 2015). Table 1 shows the particle shape and particle size parameters of the sand obtained from image analysis. All shape parameters reported in Table 1 were median values (i.e. 50%) defined from cumulative plots generated by the proprietary Windox software version 5.7.2.1, 2011, Sympatec GmbH System-Partikel-Technik from a 3-g sample. The sphericity of a particle is defined as the ratio of the equivalent perfect circle to its actual perimeter for a given area. The minimum Feret diameter divided by the maximum Feret diameter of a particle is termed aspect ratio while convexity is given by the ratio of a particle's actual area to its convex area. The parameters  $D_{10}$ ,  $D_{50}$  and  $D_{90}$ , defined for the characterisation of particle sizes are respectively the values of particle diameters at 10%, 50% and 90% on the cumulative distributions.

The flat solid selected was a microscope slide made of soda-lime-silica glass with dimensions 76 by 26 mm and thickness of 1 mm (obtained from Isolab Laborgeräte GmbH).

Table 1. Particle characteristics of Fujian sand determined from image analysis

Particle characteristics			
<i>Particle shape</i>			
Sphericity	0.8754	0.8595	0.8719
Aspect ratio	0.7201	0.7360	0.7291
Convexity	0.9200	0.9311	0.9500
<i>Particle size (<math>\mu\text{m}</math>)</i>			
$D_{10}$	153.15	226.48	493.00
$D_{50}$	206.89	374.75	589.46
$D_{90}$	280.28	459.72	757.80

#### 3.2 Coating of solids

Dimethyldichlorosilane (DMDCS) with molecular weight of 129.06 and density  $1.06 \text{ g/cm}^3$  (obtained from Acros Organics, New Jersey, USA) was used to alter the chemistry of the solids. To a 40-g sample of Fujian sand was added the following volumes ( $\mu\text{l}$ ) of DMDCS by means of a single channel pipette (Pipetman P20 from Gilson®): 5, 10, 30, 50, 100 and 200. The mixture was constantly and gently stirred for a couple of minutes. The samples were then sealed in Ziploc bags for 24 hours prior to any measurements. The microscope slide was treated by dispensing a total volume of 20  $\mu\text{l}$  on its surface and it was ensured that the top-most area was in contact with DMDCS.

### 3.3 Wettability measurements

The measurement of CAs was carried out by a goniometer (Drop Shape Analyser 25 from KRÜSS GmbH) using the sessile drop method. A 10- $\mu\text{l}$  drop was deposited on the surface of the solids at a rate of 100  $\mu\text{l min}^{-1}$ . This volume enabled a Bond number (Bo) less than 1 to be obtained, i.e. no distortions of the drop shape as a result of gravitational effects were present (Figure 4). Bo is a function of the density ( $\rho$ ) and surface tension of the liquid ( $\gamma_{lg}$ ), the gravitational constant ( $g$ ) and the base radius of the drop ( $r$ ) upon contact with the solid. For water ( $\gamma_{lg} = 0.072 \text{ N/m}$  and  $\rho = 997 \text{ kg/m}^3$ ), a  $Bo = 1$  gives a value of base radius equal to 2.71 mm.

The CCD camera incorporated in the goniometer enabled the capture of the motion of the drop as it left the automated syringe to hit the surface of the solid. As with the studies of Shang *et al.* (2008), the initial frame, taken within 50 ms after the drop touches the surface and which corresponds to the end of mechanical perturbances was extracted. The semi-automated technique developed by Saulick *et al.* (2017) was then used to evaluate the mean of 10 CAs measurements on each solid. Measurements of CAs were performed at a temperature and relative humidity of  $23 \pm 1 \text{ }^\circ\text{C}$  and  $65 \pm 5 \%$  respectively.

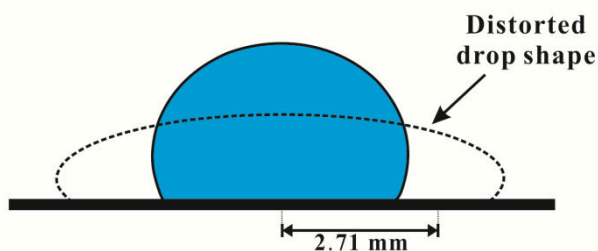


Figure 4. Drops of liquids on a surface: solid line showing no influence of gravity on the shape of the drop (Bond number,  $Bo < 1$ ) and dashed line showing distortion of the drop shape under gravity ( $Bo > 1$ ). The base radius of 2.71 mm corresponds to a  $Bo = 1$  for water.

## 4 RESULTS & DISCUSSION

Figure 5 illustrates the effect of increasing concentration of DMDCS on the CAs for the three isolated sieve fractions of Fujian sand. The concentration (%) is a ratio of the mass of DMDCS and that of Fujian sand expressed as a percentage. The standard deviations of the CAs were at most  $\pm 6^\circ$  and in line with previous studies carried out such as Bachmann *et al.* (2003). The lowest concentration used in this study, 0.01325% gave a CA of  $104.2 \pm 3.9^\circ$ ,  $108.9 \pm 4.3^\circ$  and  $104.6 \pm 5.6^\circ$  with the particle size ( $\mu\text{m}$ ): 63-212, 300-425 and 425-600 respectively. For the finest fraction, the CA increased to a maximum value of  $118.0 \pm 2.2^\circ$  at a concentration of 0.53%. The

largest CAs achieved with the 300-425 $\mu\text{m}$  and 425-600 $\mu\text{m}$  particle sizes were  $117.2 \pm 3.2^\circ$  and  $111.2 \pm 5.8^\circ$  respectively.

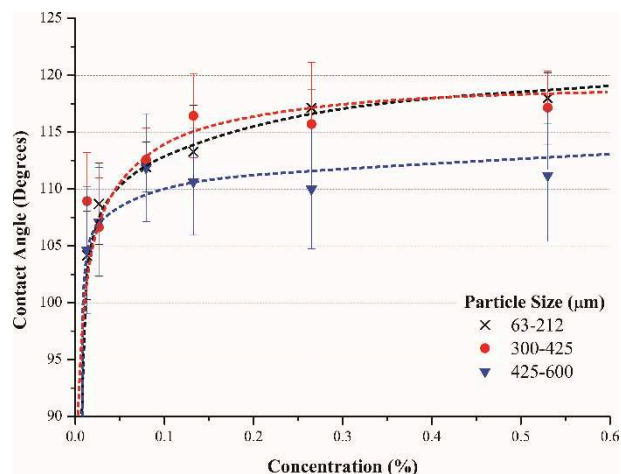


Figure 5. Contact angles as a function of particle size in samples with varying concentrations of DMDCS.

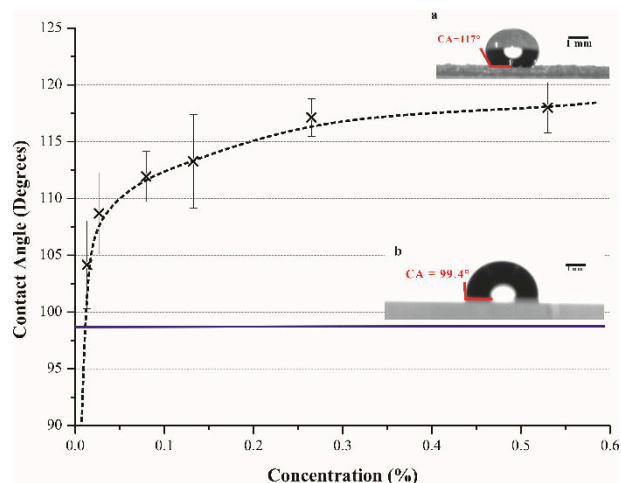


Figure 6. Variation of contact angles with increase in concentration (%) for the 63-212  $\mu\text{m}$  Fujian sand. The solid blue line represents the mean contact angle measured on the chemically treated microscope slide. Inset photographs a. and b. show drops on the Fujian sand and the microscope slide respectively.

The comparison of CA between the finest fraction of the Fujian sand and the microscope slide is shown in Figure 6. A value of  $98.5 \pm 1.5^\circ$  (blue line in Figure 6) was obtained with the microscope slide. The inset photographs in Figure 6 illustrate drops on the microscope slide and on the 63-212  $\mu\text{m}$  Fujian sand at the maximum concentration (0.53%). The contrast in the drop shapes is visually distinctive with the drop on the Fujian sand exhibiting a beaded-like outline as opposed to the drop on the microscope slide. Reasons for the discrepancies in contact angles (a maximum difference of  $20^\circ$ ) are attributed to the roughness effects at different scales. For the Fujian sand, this relates to roughness at the particle level and as an assemblage of particles which include particle size, particle shape and surface roughness. However, identifying the extent to which each of these factors singularly influence CAs is a challenge.

The calculated values of the roughness ratio,  $r$  assuming  $CA_Y$  equal to  $98.5^\circ$  (the CA measured on the

microscope slide) with the Fujian sand treated at concentration of 0.53% gave values of 3.175, 3.088 and 2.446 with the particle sizes ( $\mu\text{m}$ ) 63-212, 300-425 and 425-600 respectively. An increase in  $r$  as the particle sizes became finer corresponded to an increase in measured CAs.

## 5 CONCLUSIONS

The influence of the particle characteristics of granular solids on water repellency has been shown by comparing 3 isolated fractions of a sand. The largest contact angle was achieved with the finest fraction. Comparison between the microscope slide, made water repellent by chemical treatment with the 63-212  $\mu\text{m}$  sand fraction showed a maximum difference of  $20^\circ$  in contact angles. This difference was attributed to the particle size, particle shape and surface roughness of the particles.

The study showed that water repellency in granular solids such as soils can be gauged by alternative means beyond just chemistry. This offers the advantage of deploying such material in engineering applications by being less reliant on coatings imparted from chemical treatments and potentially offering longer durability of water repellent granular solids.

## 6 ACKNOWLEDGEMENTS

The authors would like to thank Dr. S. K. Woche for her help in acquiring the ESEM images. Financial support provided by the General Research Fund, Research Grants Council, Hong Kong (17221016 and 17203417) and HKU seed fund for basic research (201406159004 and 201511159205) are acknowledged.

## 7 REFERENCES

- Bachmann, J., Woche, S.K., Goebel, M.O., Kirkham, M.B. and Horton, R. 2003. Extended methodology for determining wetting properties of porous media. *Water Resources Research* 39(12): 1353.
- Bachmann, J. and McHale, G. 2009. Superhydrophobic surfaces: a model approach to predict contact angle and surface energy of soil particles. *European Journal of Soil Science* 60(3): 420-430.
- Byun, Y.H., Tran, M.K., Yun, T.S. and Lee, J.S. 2011. Strength and stiffness characteristics of unsaturated hydrophobic granular media. *Geotechnical Testing Journal* 35(1): 193-200
- Cassie, A.B.D. and Baxter, S. 1944. Wettability of porous surfaces. *Transactions of the Faraday Society* 40: 546-551.
- Ellies, A., Ramirez, C. and Mac Donald, R. 2005. Organic matter and wetting capacity distribution in aggregates of Chilean soils. *Catena* 59(1): 69-78.
- Hallett, P.D. and Young, I.M. 1999. Changes to water repellence of soil aggregates caused by substrate-induced micro-

- bial activity. *European Journal of Soil Science* 50(1): 35-40.
- Israelachvili, J.N. 2011. Intermolecular and surface forces. Academic press.
- King, P.M. 1981. Comparison of methods for measuring severity of water repellence of sandy soils and assessment of some factors that affect its measurement. *Soil Research* 19(3): 275-285.
- Kwok, D.Y. and Neumann, A.W. 1999. Contact angle measurement and contact angle interpretation. *Advances in Colloid and Interface Science* 81(3): 167-249.
- Lourenço, S.D.N., Saulick, Y., Zheng, S. Kang, H., Liu, D., Lin, H. and Yao, T. 2018. Soil wettability in ground engineering: fundamentals, methods, and applications. *Acta Geotechnica* 13(1): 1-14.
- Rodriguez, M.A., Rubio, J., Rubio, F., Liso, M.J. and Oteo, J.L. 1997. Application of inverse gas chromatography to the study of the surface properties of slates. *Clays and Clay Minerals* 45(5): 670-680.
- Saulick, Y., Lourenço, S.D.N. and Baudet, B.A. 2017. A Semi-Automated Technique for Repeatable and Reproducible Contact Angle Measurements in Granular Materials using the Sessile Drop Method. *Soil Science Society of America Journal* 81(2): 241-249.
- Shang, J., Flury, M., Harsh, J.B. and Zollars, R.L. 2008. Comparison of different methods to measure contact angles of soil colloids. *Journal of Colloid and Interface Science* 328(2): 299-307.
- Wenzel, R.N. 1936. Resistance of solid surfaces to wetting by water. *Industrial & Engineering Chemistry* 28(8): 988-994.
- Yang, J. and Luo, X.D. 2015. Exploring the relationship between critical state and particle shape for granular materials. *Journal of the Mechanics and Physics of Solids* 84: 196-213.